Pergamon

Bioorganic & Medicinal Chemistry 8 (2000) 497–506

BIOORGANIC & MEDICINAL CHEMISTRY

Acetylcholinesterase Inhibitors for Potential Use in Alzheimer's Disease: Molecular Modeling, Synthesis and Kinetic Evaluation of 11*H*-Indeno-[1,2-*b*]-quinolin-10-ylamine Derivatives

Angela Rampa, Alessandra Bisi, Federica Belluti, Silvia Gobbi, Piero Valenti,* Vincenza Andrisano, Vanni Cavrini, Andrea Cavalli and Maurizio Recanatini

Department of Pharmaceutical Sciences, University of Bologna, Via Belmeloro 6, I-40126 Bologna, Italy

Received 17 February 1999; accepted 14 September 1999

Abstract—Continuing our work on tetracyclic tacrine analogues, we synthesized a series of acetylcholinesterase (AChE) inhibitors of 11*H*-indeno-[1,2-*b*]-quinolin-10-ylaminic structure. Selected substituents were placed in synthetically accessible positions of the tetracyclic nucleus, in order to explore the structure–activity relationships (SAR) and the mode of action of this class of anticholinesterases. A molecular modeling investigation of the binding interaction of the lead compound (**1a**) with the AChE active site was performed, from which it resulted that, despite the rather wide and rigid structure of **1a**, there may still be the possibility to introduce some small substituent in some positions of the tetracycle. However, from the examination of the experimental IC_{50} values, it derived that the indenoquinoline nucleus probably represents the maximum allowable molecular size for rigid compounds binding to AChE. In fact, only a fluorine atom in position 2 maintains the AChE inhibitory potency of the parent compound, and, actually, increases the AChE-selectivity with respect to the butyrylcholinesterase inhibition. By studying the kinetics of AChE inhibition for two representative compounds of the series, it resulted that the lead compound (**1a**) shows an inhibition of mixed type, binding to both the active and the peripheral sites, while the more sterically hindered analogue **2n** seems to interact only at the external binding site of the enzyme. This finding seems particularly important in the context of Alzheimer's disease research in the light of recent observations showing that peripheral AChE inhibitors might decrease the aggregating effects of the enzyme on the β-amyloid peptide (βA).

Introduction

One of the few undisputed evidences in the neuropathology of the Alzheimer's disease (AD) is the loss of cholinergic neurons occurring in different areas of the central nervous system (CNS), mainly the cerebral cortex and the hyppocampus. This loss of cholinergic innervation is the ultimate cause of the cognitive and behavioral abnormalities that characterize AD, and it is not a surprise that the early pharmacological approaches to the treatment of the AD patients were aimed at increasing the availability of the cholinergic neurotransmitter acetylcholine (ACh). On this basis, the *cholinergic hypothesis*[1,2] became the leading strategy for the development of AD drugs, even if today other approaches are also being followed in the search for agents able to treat and/or prevent the disease.[3]

Compounds able to increase the levels of ACh can be either cholinergic receptor ligands or acetylcholinesterase (AChE) inhibitors, but the best results up to date have been achieved with the latter type of agents, some of which are currently marketed or are in advanced clinical trial for the symptomatic treatment of AD.[4]

Tacrine was the first AChE inhibitor to be launched as an AD drug,[5] but, together with evidences of beneficial effects on the AD symptoms, it showed several adverse side effects which in some cases made its use problematic.[3] Also for this reason, many other AChE inhibitors were studied (from which the second generation drug Donepezil was developed) and research efforts still continue aimed at improving the pharmacological profile of the prototypes.

In a previous paper,[6] we reported the synthesis and the biological evaluation of some AChE inhibitors related to tacrine, where the tricyclic structure of the 1,2,3,4-tetrahydroacridine nucleus was expanded to a tetracyclic one (**1a–d**). The inhibition of AChE was tested

*Corresponding author. Tel.: +39-51-209-9701; fax: +39-51-209-9734; e-mail: pvalenti@alma.unibo.it

0968-0896/00/$ - see front matter
PII: S0968-0896(99)00306-5

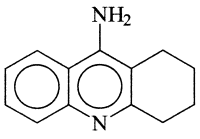

Tacrine

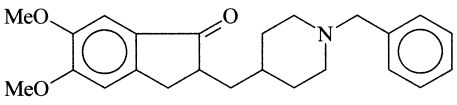

Donepezil

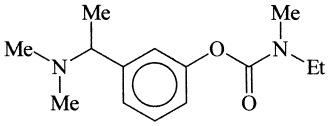

Rivastigmin (ENA-713)

both on the isolated enzyme and in rat brain cortex homogenate, and the respective IC_{50} values correlated well between each other indicating that the inhibitory activity is maintained in the target biological system. From that study, it resulted that the methylene-bridged molecule (**1a**) has an inhibitory potency of the same level as tacrine and a better selectivity with respect to the butyrylcholinesterase (BuChE) inhibition.

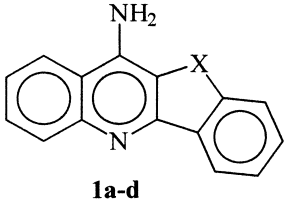

	X
1a	CH_2
1b	CH_2CH_2
1c	OCH_2
1d	SCH_2

1a-d

Independently, McKenna et al.[7] published a study on some tetracyclic derivatives of tacrine bearing the same general structure as shown above and characterized by various X bridges and, eventually, by some substituent in different positions of the polycyclic nucleus. Also these authors individuated the monomethylene derivative (**1a**) as the most promising one in view of further development.

Based on the above premises, we decided to continue our work on the tetracyclic tacrine analogues in order to explore the structure–activity relationships (SAR) and the mode of action of this class of AChE inhibitors. In the present paper, we report a molecular modeling investigation of the binding interaction of the lead compound (**1a**) with the AChE active site, a SAR study of the series based on a number of newly synthesized compounds (Table 1), and the kinetic assessment of the mode of action of two representative members of the class. The last issue seems particularly important in the light of recent observations reported by Inestrosa et al.,[8] who showed that AChE inhibitors might decrease the aggregating effects of the enzyme on the β-amyloid peptide (βA). Actually, βA is the main component of the senile plaques found in AD brain and any compound able to inhibit its aggregation might be regarded as potentially useful in view of a pharmacological treatment of the disease.[9]

Table 1. AChE and BuChE inhibitory activity (IC_{50}) of the 11*H*-indeno-[1,2-*b*]-quinolin-10-ylamine derivatives

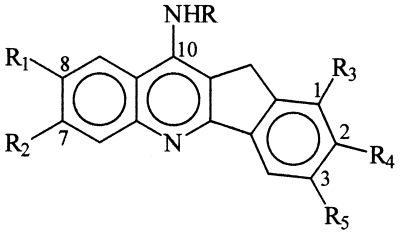

No.	R	R_1	R_2	R_3	R_4	R_5	$IC_{50} \pm$ SE AChE (μM)	$IC_{50} \pm$ SE BuChE (μM)
1a[a]	H	H	H	H	H	H	0.68 ± 0.02	4.7 ± 0.1
2a	H	NO_2	H	H	H	H	> 100	nd[b]
2b	H	NH_2	H	H	H	H	5.9 ± 0.3	nd
2c	H	H	NO_2	H	H	H	67.5 ± 5.9	nd
2d	H	H	NH_2	H	H	H	29.0 ± 0.9	nd
2e	H	H	Cl	H	H	H	6.5 ± 0.7	nd
2f	H	H	F	H	H	H	1.2 ± 0.1	5.7 ± 0.3
2g	H	H	H	OCH_3	H	H	1.6 ± 0.1	3.0 ± 0.6
2h	H	H	H	H	OCH_3	H	6.5 ± 0.2	nd
2i	H	H	H	H	H	OCH_3	4.3 ± 0.3	nd
2j	H	H	H	CH_3	H	H	3.9 ± 0.2	nd
2k	H	H	H	H	H	CH_3	4.6 ± 0.1	nd
2l	H	H	H	H	F	H	0.43 ± 0.02	7.1 ± 0.3
2m	H	H	H	H	Cl	H	5.4 ± 0.3	nd
2n	$CH_2C_6H_5$	H	H	H	H	H	7.1 ± 0.1	0.5 ± 0.07
2o	CH_3	H	H	H	H	H	1.3 ± 0.05	1.6 ± 0.1
2p	C_7H_{15}	H	H	H	H	H	4.3 ± 0.4	nd
Tacrine[a]							0.25 ± 0.01	0.05 ± 0.002

[a]Ref. 6.
[b]Not determined.

Methods

Molecular modeling

The putative binding mode of **1a** inside the AChE active site was studied by performing a molecular dynamics (MD) simulation on an optimized docking model of the enzyme–inhibitor complex. Using the X-ray structure of the AChE–tacrine complex[10] as a starting template, we built an initial three-dimensional model of **1a** hosted in the human AChE gorge, by simply modifying the structure of tacrine to obtain that of **1a**. The Phe330 residue of the protein sequence was changed to Tyr, which is the only mutated residue in the active site region of the human enzyme with respect to that from *Torpedo californica*.[11] After optimization, the complex was subjected to an MD simulation aimed at finding the most favorable location of the inhibitor within the binding pocket.

Chemistry

The compounds reported in Table 1 were prepared as shown in Schemes 1 and 2. In Scheme 1, the synthesis of compounds **2a–n** is illustrated. Compounds **2a**, **2c** and **2e–m** were prepared by condensation of the selected aminobenzonitrile with the selected indanone in the presence of $ZnCl_2$. Compounds **2b** and **2d** were obtained by catalytic (Pd/C) hydrogenation of **2a** and **2c**, respectively. Compound **2n** was prepared starting from **1a** by refluxing in DMF with benzaldehyde and subsequent reduction with $NaBH_4$ of the obtained Schiff base. The aminobenzonitriles not commercially available were prepared starting from anthranilic acids by treatment with thionyl chloride, ammonia, and, finally, P_2O_5.

Compounds **2o** and **2p** were prepared as shown in Scheme 2, by heating anthranilic acid and indanone to give the chloro-derivative **3**, which was treated with methylamine or heptylamine to yield the desired compounds.

Enzyme inhibition

The inhibitory activity of the newly synthesized compounds against AChE was studied using the method of Ellmann et al.[12] to determine the rate of hydrolysis of acetylthiocholine (ATCh) in the presence of the inhibitor. The IC_{50} values reported in Table 1 were obtained by extrapolation from the inhibition curves. The selectivity of some representative compounds was also tested by determining their inhibitory activity against BuChE. The results are reported in Table 1 as IC_{50} values.

Moreover, the binding mode of both the series lead (**1a**) and **2n** was investigated to assess their possibility of binding to the AChE peripheral site. As reported by Inestrosa et al.,[8] this external site is presumably involved in the AChE–βA-inhibitor interaction and compounds binding to it were shown to decrease the aggregation of βA. We determined the K_i (Table 2) of the selected compounds and of two reference compounds as well, which are known to behave differently as regards the AChE binding sites: tacrine and propidium. From the analysis of the inhibition plots, the different binding modes could then be hypothesized.

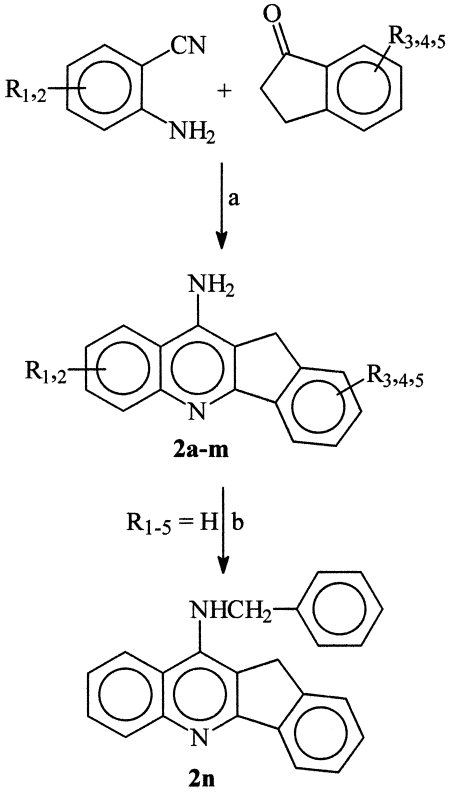

Scheme 1. Reagents: (a) $ZnCl_2$ reflux; (b) (1) benzaldehyde reflux, (2) $NaBH_4$.

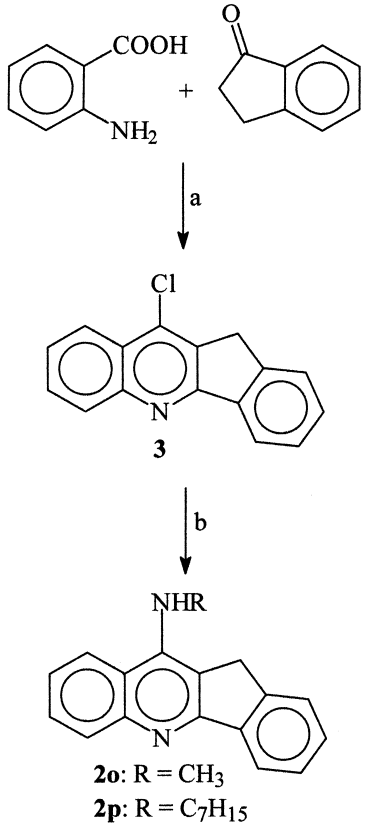

Scheme 2. Reagents: (a) $POCl_3$ reflux; (b) RNH_2 reflux.

Results and Discussion

Three-dimensional model of the inhibitor–active site interactions

The position of tacrine inside the active site gorge of the *T. californica* AChE was determined by Sussman et al. by means of an X-ray crystallographic analysis.[10] From that study, it resulted that 9-amino-1,2,3,4-tetrahydroacridine is bound to the enzyme through two main interactions, namely a π-stacking with the indolic ring of Trp84 and a hydrogen bond between the acridinic protonated nitrogen and the His440 carbonyl oxygen; moreover, one aminic hydrogen is H-bonded to a water molecule. In Figure 1a, the X-ray-determined binding mode of tacrine (magenta) is shown.

In Figure 1b, the position of **1a** (orange) bound to the AChE active site is shown as it resulted after 140 ps of MD simulation. Some surrounding aminoacid residues and water molecules are also shown; hydrogen bonds are indicated as yellow dotted lines.

The main interaction between **1a** and AChE is a double π–π interaction involving the tetracyclic nucleus and both Trp84 and Tyr330. The three rings lie on almost perfectly parallel planes and they are rather tightly packed, as indicated by the average distances between **1a** and both the indolic and the phenolic rings: 3.2 and 3.3 Å, respectively.

It appears from Figure 1b that the ligand does not make any direct hydrogen bond with the enzyme, even if the phenolic oxygen of Tyr334 is in a favorable position to bind the aminic hydrogen of **1a**. Actually, during the MD simulation, a H-bond between the phenolic O and the aminic N is recorded for 25% of the time. On the other hand, two water molecules are hydrogen-bonded to the aminic group of **1a** and contribute to stabilize its position by creating a H-bond array involving the side chains of Asp72 and Tyr330. The acridinium proton is bound to the water molecule bridging His440 and Glu199.

Comparing the positions of the two inhibitors—tacrine (Fig. 1a) and indenoquinoline **1a** (Fig. 1b)—docked into the AChE active site, it appears that both molecules arrange themselves in order to take advantage at best of their possibility to establish π–π interactions. An MD simulation carried out on the tacrine–AChE complex (data not shown) confirms the orientation obtained from the X-ray analysis. In search for an optimal orientation, **1a** rotated around its perpendicular axis and changed the H-bond interactions with respect to tacrine. This resulted in the 'sandwich' interaction depicted in Figure 1b and in the loss of the H-bond between the acridinic H and the His440 carbonyl O. The cavity containing the tetracyclic nucleus is lined by Ile439, Tyr330, Tyr334, Trp432 and Tyr442 (not shown) on the left side of the picture and by Ser122 and Tyr121 (not shown) on the right side. Despite the rather wide and rigid structure of **1a**, it seems that there may still be the possibility to introduce some small substituent in various positions of the tetracyclic nucleus, specially on the aryl ring facing an almost empty zone in correspondence to positions 1, 2 and 3 of **1a**.

Structure–activity relationships for the AChE inhibition

Substituents were introduced in the synthetically accessible positions of the aryl rings of **1a** as well as on the primary amino-group, in order to explore the SAR of the series. The structural characteristics of the new derivatives and the AChE inhibition data expressed as IC_{50} values are shown in Table 1.

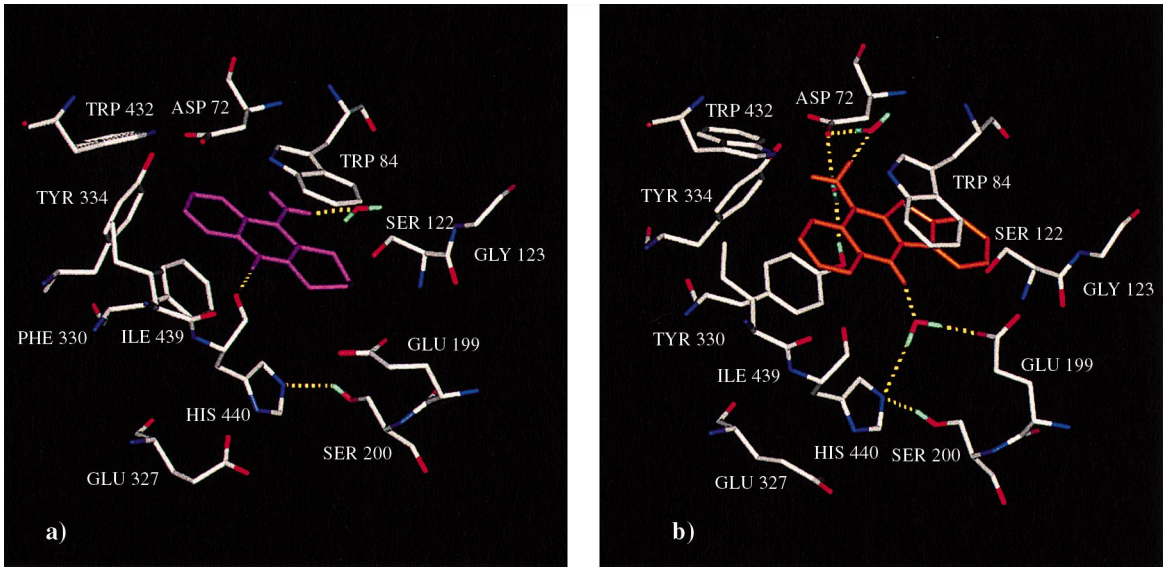

Figure 1. Interactions of tacrine ((a), magenta) and of the 11*H*-indeno-[1,2-*b*]-quinolin-10-ylamine **1a** ((b), orange) with some selected aminoacid

For positions 7 and 8 of the indenoquinoline nucleus, corresponding to positions 6 and 7, respectively, of tacrine, electronically active substituents were chosen, considering their possible effect on the protonation of the quinolinic N atom, and on the basis of the known SAR of 9-aminoacridinic AChE inhibitors as well. In fact, Schutske et al.[13] studied a small set of 6- and 7-substituted 9-amino-1,2,3,4-tetrahydroacridin-1-ols and concluded that the inhibitory activity of the unsubstituted parent compound can be increased by introducing substituents like F or Cl in position 6 and that such an increase of potency cannot be ascribed to lipophilicity alone. In another work, Wlodek et al.[14] analyzed by theoretical methods the effects of a Cl atom in the 6 position of tacrine and found that this substituent increases the binding strength to AChE probably due to its electron-withdrawing effect.

We introduced the electron-attracting groups NO_2 (in positions 8 and 7, compounds **2a** and **2c**, respectively), Cl (in position 7, compound **2e**), and F (in position 7, compound **2f**), and the electron-donating NH_2 group (in positions 8 and 7, compounds **2b** and **2d**, respectively). All the substituents in both the studied positions caused a decrease of AChE inhibitory activity, with the strongest electron-attracting group (NO_2 in compounds **2a** and **2c**) giving the most relevant drop of potency. The electron-donor NH_2 in the same positions (compounds **2b** and **2d**) also had an unfavorable effect on activity, even if not at the level of the NO_2: compound **2b** ($R_1 = NH_2$) was about nine times less potent than the parent molecule **1a**. Halogens in position 7 (corresponding to tacrine's position 6) reduced the inhibitory activity: Cl (compound **2e**) about 10 times, F (compound **2f**) less than two times.

Considering the above results, it appears evident that the introduction of substituents in positions 7 (R_2) and 8 (R_1) of the tetracyclic nucleus is detrimental for the AChE inhibitory activity. A direct explanation of this effect might be that atoms or groups bigger than hydrogen (F is the best tolerated) impair either the inhibitor–enzyme binding interaction, or the dynamic process of reaching the binding site, or both. The electronic characteristics of the substituents might have an effect on the protonation of the nuclear N atom. The IC_{50} data relative to compounds **2a–d** point to a definitely negative effect of electron attraction (it reduces the N basicity) and to a less negative effect of electron donation (it stabilizes the positive charge). Remarkably, the relative potencies of compounds **2b** and **2d** parallel their electron donating ability as estimated by the NH_2 Hammett's σ constants for the positions *para* (position 8, **2b**) and *meta* (position 7, **2d**) with respect to the nuclear quinolinic nitrogen: -0.66 and -0.16, respectively.[15]

As regards the phenyl ring fused to the pentaatomic cycle, substituents were placed in accessible positions of it, to probe their steric tolerability. Methoxy groups were introduced in 1, 2 and 3 (compounds **2g–i**), methyl groups in 1 and 3 (compounds **2j** and **2k**) and halogens in 2 (compounds **2l** and **2m**). Note that the Cl atom in 2 is sterically equivalent to a methyl group (molar refractivity values are 0.56 and 0.60, respectively[15]). All the latter derivatives except **2l** show a similar AChE inhibitory activity, from about two to about 10 times lower than the unsubstituted compound **1a**. Compound **2l** ($R_4 = F$) is slightly more active than **1a**. These results again point out a detrimental steric effect exerted by substituents introduced on the tetracyclic nucleus, whereas the small fluorine atom is the only favorable substitution in all the series. However, the improvement of activity is small and it might be explained with an action on the π electron cloud of the aryl ring, that is involved in stacking interactions with some aromatic residue on the enzyme surface (see previous section).

Finally, the primary amino group was modified by introducing on it a benzyl- (compound **2n**), methyl- (compound **2o**), or heptyl-substituent (compound **2p**), which had been already tested in the corresponding position of 1,2,3,4-tetrahydro-9-aminoacridines[16] and 1,2,3,4-tetrahydro-9-aminoacridin-1-ols.[13] Moreover, from a recent comparative QSAR analysis[17] performed on a series of AChE inhibitors, it emerged that the inhibitory potency of acridinic derivatives is sensitive to the length of the substituent in position 9. Consequently, we chose three substituents of varying length as benzyl ($L = 4.62$), methyl ($L = 2.87$), and heptyl ($L = 9.03$).[15] It appears from the data reported in Table 1 that compounds **2n–p** are less active than the reference compound **1a**, but, interestingly, their IC_{50} values are in agreement with the results of the mentioned QSAR analysis. In fact, it resulted from the latter that substituents characterized by an L value around 5 give less potent inhibitors than substituents with L values lower or higher than 5:[17] this seems to be the case of compounds **2n–p**, with the benzyl-substituted derivative (**2n**, $L = 4.62$, $IC_{50} = 7.1 \pm 0.1$ μM) slightly less active than both the methyl- (**2o**, $L = 2.87$, $IC_{50} = 1.3 \pm 0.05$ μM) and the heptyl- (**2p**, $L = 9.03$, $IC_{50} = 4.3 \pm 0.4$ μM) substituted ones.

The AChE/BuChE selectivity of the substituted indenoquinolines was investigated by measuring the BuChE inhibitory activity of **2f**, **2g**, **2l** and **2o**, which are the most potent AChE inhibitors of the series. From the IC_{50} data reported in Table 1, it results that the introduction of the F atom in position 2 (compound **2l**) allowed us to improve the selectivity of the parent compound **1a**, that, in turn, was much better than that of tacrine. In fact, the AChE/BuChE selectivity ratios are 16.5 for **2l** and 6.9 for **1a**, while tacrine is BuChE-selective. The remaining compounds tested for the BuChE inhibition are slightly AChE-selective. Compound **2n** ($R = CH_2C_6H_5$) was also tested for the AChE/BuChE selectivity and it resulted more active as a BuChE inhibitor than as an AChE inhibitor. This feature, however, might be explained by the finding that **2n** should not be able to reach the active site of AChE inside the gorge, while it might reach the BuChE's one due to the lack of any external binding site in the latter enzyme (see discussion below).

In summary, what emerges from the present SAR analysis is that the indenoquinoline nucleus probably represents the maximum allowable molecular size for rigid compounds binding to AChE. In fact, despite the

different physicochemical properties, any substituent on the rings except for the fluorine atom exerts a detrimental effect on the AChE inhibitory activity. On the other hand, AChE inhibitors unable (in all or in part) to penetrate inside the active site gorge may have more chances to bind at the enzyme peripheral site, which could represent an useful feature in the context of research for AD affecting agents.

Mechanism of AChE inhibition

AChE possesses an active site at which substrates like ACh and ATCh are hydrolyzed and a peripheral anionic site, which is spatially distinct from the active center and where selective inhibitors can bind with high affinity and specificity.[18] Hydrolysis of ACh (and ATCh) proceeds through the formation of an acyl–enzyme intermediate, and inhibitors can affect steady-state kinetics by association with the transient acyl-intermediate in addition to the free enzyme and enzyme–substrate complex.[19] As the association of AChE with βA and the formation of amyloid fibrils can be inhibited by peripheral anionic site ligands such as propidium,[8] inhibitors capable of binding to the acyl–enzyme and to the peripheral site (postulated to be Trp279, *T. californica* numbering[20]) can be of utmost interest in view of a potential use for the treatment of AD.

Based on the above considerations and on the hypothesis that the rather wide shape of molecules like **1a** and its analogues might impair the entrance into the AChE gorge and favor the binding at an external site, we studied the steady state kinetics of two representative compounds of the series, the lead **1a** and the largest derivative **2n**. The graphical analysis of steady state inhibition data can give information on the binding mode of the selected compounds, and allow the assessment of their K_i as well.

The inhibition of AChE by **1a** and **2n** was very fast and not time dependent, as the 50% enzyme inactivation produced by the respective IC_{50} concentrations following 1 min incubation was not significantly ($P > 0.01$) different from the inhibition observed up to 40 min incubation. The graphical analysis of the inhibition data for **1a** and **2n** in comparison with tacrine and propidium is shown in Figure 2, whereas the estimates of the inhibition constants K_i are reported in Table 2.

Reciprocal plots (Lineweaver–Burk plots) describing **1a** and tacrine inhibition show both increasing slopes and increasing intercepts with higher inhibitor concentration (Fig. 2a and b, respectively). This pattern indicates mixed inhibition, arising from significant inhibitor interaction with both the free enzyme and the acetylated enzyme. [21]

Table 2. AChE inhibition constants of some selected derivatives

Compound	$K_i \pm$ SE (μM)
1a	0.210 ± 0.036
Tacrine	0.151 ± 0.016
2n	7.50 ± 1.15
Propidium	7.14 ± 1.50

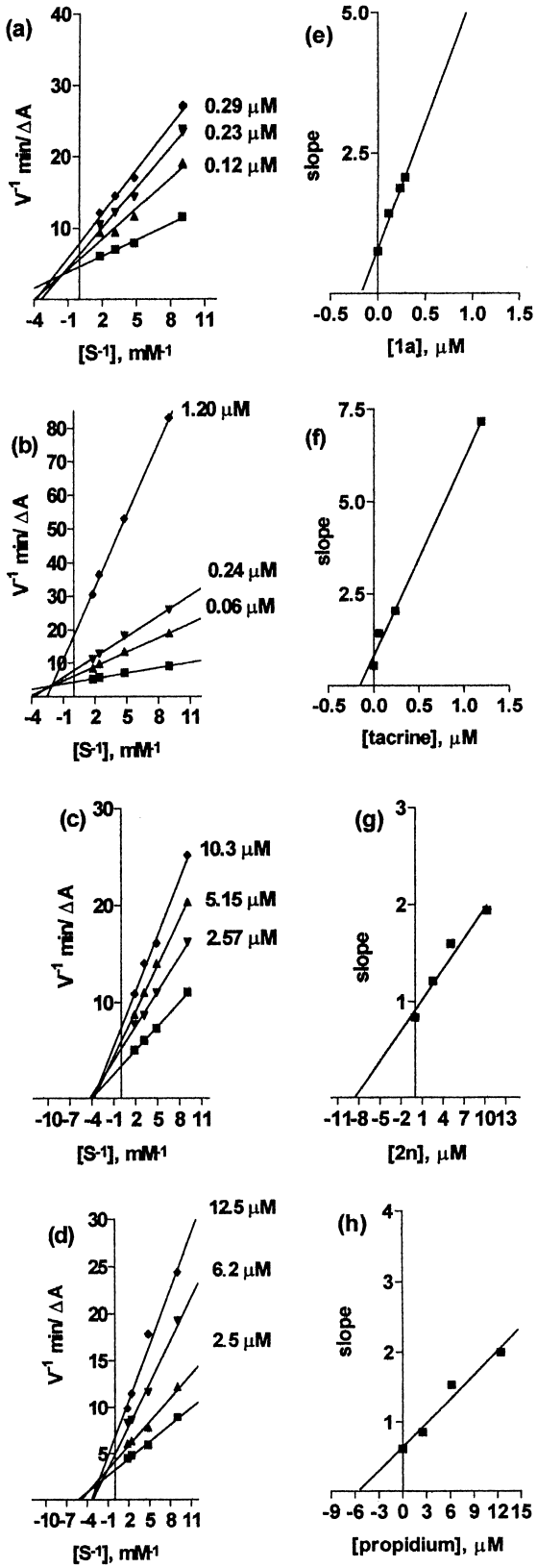

Figure 2. Steady state inhibition by **1a** (a, e), tacrine (b, f), **2n** (c, g) and propidium (d, h) of AChE hydrolysis of ATCh; (a–d) reciprocal plots of initial velocity and substrate concentration: the plots show mixed-type inhibition for **1a** (a) and tacrine (b), and non competitive inhibition for **2n** (c) and propidium (d); (e–g) replots of the reciprocal plots versus inhibitor concentration: in each plot, the x axis intercept represents the K_i of the inhibitor.

Replots of the slope versus the inhibitor concentration (Fig. 2e and f) give the estimates of the competitive inhibition constants reported in Table 2. Compound **1a** shows a K_i value very similar to tacrine and the same pattern in the graphical representation. So as tacrine,[22] **1a** looks keen to bind to the peripheral anionic site as a secondary binding site.

In the reciprocal plots of Figure 2c, lines crossing the x axis in the same point reveal unchanged K_m and decreased V_{max} at increasing inhibitor concentrations. This is a typical trend for non competitive inhibition and indicates that the inhibitor (in this case **2n**) binds with high affinity to a site different from the catalytic one.[21] Propidium has been described as a ligand selective for the AChE peripheral site,[18] and shows the same behavior as **2n** at the lowest inhibitor concentration (2.5 μM, Fig. 2d).

As non competitive type of inhibition can be either pure or partial, the linear instead of hyperbolic slope replot shown in Figure 2g was associated with a pure non competitive inhibition. However, being this plot linear also for a pure competitive type of inhibition, the Dixon plot $1/V$ versus inhibitor concentration was studied for **2n** (Fig. 3a). The replot of slopes versus $1/[S]$ was then obtained (Fig. 3b), in which the straight line does not pass through the origin as it would do in case of a pure competitive inhibition. These results probably reflect a conformational change in the enzyme caused by **2n** binding to the enzyme–substrate complex, yielding a non productive AChE–ATCh–**2n** complex.

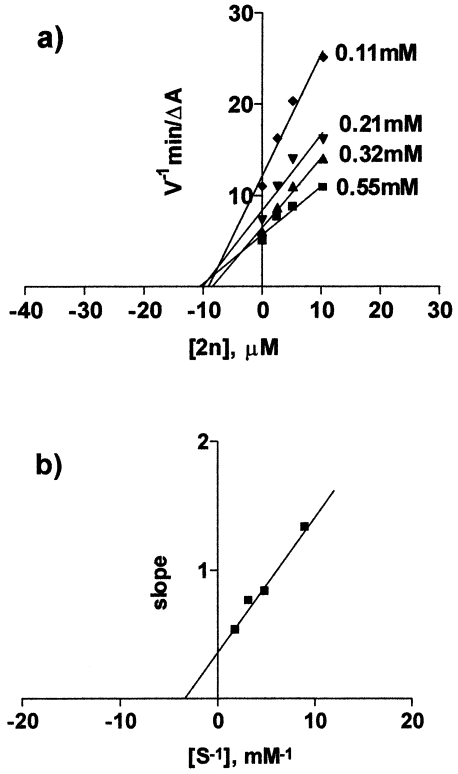

Figure 3. (a) Dixon plots representing reciprocal of initial AChE velocity versus **2n** concentration at four substrate concentrations as indicated in the graph; (b) secondary replot of the Dixon plot slopes versus reciprocal of the substrate concentrations ($r^2 = 0.9800$).

From the above analysis of the kinetics data it results that the lead compound of the series **1a** behaves like tacrine as regards its binding mode to AChE: it is able to penetrate into the active site gorge, and it binds also to the peripheral site, showing an inhibition of mixed type. On the other hand, **2n** seems to parallel the propidium binding mode, interacting only at the external site of the enzyme, and this feature might be a consequence of the increased steric hindrance provided by the benzyl group attached to the 10-amino-function of the indenoquinoline nucleus.

The hypothesis of an external binding for **2n** is also consistent with its BuChE/AChE selectivity data (Table 1). In fact, the IC_{50} values for the BuChE and AChE inhibitory activities might reflect the ability of this compound to penetrate into the BuChE active site cavity, but not into the AChE gorge. The structural reason for this might be that the tryptophan residue Trp279 at the entrance of the gorge is present in AChE, but absent in BuChE.[20]

Conclusion

The SAR of a series of AChE inhibitors structurally derived from the 11*H*-indeno-[1,2-*b*]-quinolin-10-ylamine were explored by inserting selected substituents in synthetically accessible positions of the tetracyclic nucleus. The putative interactions of the lead compound **1a** with the enzyme binding site inside the AChE gorge were studied, in order to qualitatively evaluate the feasibility of such structural modifications. Most of the new analogues resulted less potent inhibitors than the lead **1a** independently on the different electronic properties of the substituents, suggesting that steric hindrance could limit the access to the enzyme binding site. On the other hand, compound **2l** was slightly more potent as an AChE inhibitor than **1a**, and it was also definitely more selective for AChE with respect to BuChE.

After a deeper kinetic evaluation, it was shown that the active site inside the AChE gorge is not the only available binding site for these molecules, and that a peripheral site can significantly contribute to the overall inhibitor–enzyme interaction. Compound **1a** displayed a mixed type of inhibition similar to that of tacrine, while compound **2n** was shown to be able to bind only to the peripheral site analogously to propidium. The latter finding is of particular interest in view of further development of compound **2n** as an inhibitor of the aggregation of βA, a critical target in the research for an effective AD treatment.

Experimental

Chemistry

All melting points were determined in open glass capillaries using a Büchi apparatus and are uncorrected. ^{1}H NMR spectra were recorded in $CDCl_3$ solution on a Varian Gemini 300 spectrometer with Me_4Si as internal

standard. Wherever analyses are only indicated with element symbols, analytical results obtained for those elements are within 0.4% of the theoretical values. Compounds were named following IUPAC rules applied by AUTONOM, a PC software for systematic names in organic chemistry, Beilstein Institut and Springer.

Preparation of compounds 2a, 2c and 2e–m. A mixture of selected anthranilonitrile (0.01 mol), selected indanone (0.01 mol) and dry $ZnCl_2$ (3 g) was heated at 120–130 °C for 3 h. After cooling, the reaction mixture was treated with water and the separated solid, collected by filtration, was crystallized from ethanol.

2a: Yield 80%, mp 177–180 °C. ^{1}H NMR δ 3.9 (s, 2H, CH_2), 7.5–8.4 (m, 8H, Ar, NH_2), 9.4 (s, 1H, Ar). MS: *m*/*z* (rel. abundance) 277 ($M^{\cdot+}$, 100), 247 (18), 231 (38), 204 (23). Anal. ($C_{16}H_{11}N_3O_2$): C, H, N.

2c: Yield 40%, mp 208–211 °C. ^{1}H NMR δ 3.9 (s, 2H, CH_2), 7.2–8.6 (m, 9H, Ar, NH_2). MS: *m*/*z* (rel. abundance) 277 ($M^{\cdot+}$, 100), 231 (53), 204 (15), 102 (6). Anal. ($C_{16}H_{11}N_3O_2$): C, H, N.

2e: Yield 90%, mp >300 °C. ^{1}H NMR δ 3.95 (s, 2H, CH_2), 7.5–8.5 (m, 9H, Ar, NH_2). MS: *m*/*z* (rel. abundance) 266 ($M^{\cdot+}$, 100), 231 (22), 133 (10), 115 (5). Anal. ($C_{16}H_{11}ClN_2$): C, H, N.

2f: Yield 90%, mp >300 °C. ^{1}H NMR δ 3.95 (s, 2H, CH_2), 7.5–8.6 (m, 7H, Ar), 8.8 (broad 2H, NH_2). MS: *m*/*z* (rel. abundance) 250 ($M^{\cdot+}$, 100), 125 (19), 36 (27), 32 (32). Anal. ($C_{16}H_{11}FN_2$): C, H, N.

2g: Yield 60%, mp 253–255 °C. ^{1}H NMR δ 3.75 (s, 2H, CH_2), 3.95 (s, 3H, OCH_3) 7.1–8.4 (m, 9H, Ar, NH_2). MS: *m*/*z* (rel. abundance) 262 ($M^{\cdot+}$, 100), 247 (39), 231 (53), 219 (20). Anal. ($C_{17}H_{14}N_2O$): C, H, N.

2h: Yield 60%, mp >300 °C. ^{1}H NMR δ 4.9 (s, 3H, OCH_3), 4.95 (s, 2H, CH_2), 7.2–8.5 (m, 9H, Ar, NH_2). MS: *m*/*z* (rel. abundance) 262 ($M^{\cdot+}$, 100), 247 (16), 231 (25), 219 (64). Anal. ($C_{17}H_{14}N_2O$): C, H, N.

2i: Yield 60%, mp 282–285 °C. ^{1}H NMR δ 3.8 (s, 3H, OCH_3), 3.9 (s, 2H, CH_2), 7.1–8.5 (m, 9H, Ar, NH_2). MS: *m*/*z* (rel. abundance) 262 ($M^{\cdot+}$, 100), 247 (58), 231 (56), 219 (55). Anal. ($C_{17}H_{14}N_2O$): C, H, N.

2j: Yield 75%, mp >300 °C. ^{1}H NMR δ 2.4 (s, 3H, CH_3), 3.8 (s, 2H, CH_2), 7.2–8.3 (m, 9H, Ar, NH_2). MS: *m*/*z* (rel. abundance) 246 ($M^{\cdot+}$, 100), 231 (56), 115 (7), 77 (11). Anal. ($C_{17}H_{14}N_2$): C, H, N.

2k: Yield 80%, mp 277–280 °C. ^{1}H NMR δ 2.4 (s, 3H, CH_3), 3.9 (s, 2H, CH_2), 7.2–8.4 (m, 9H, Ar, NH_2). MS: *m*/*z* (rel. abundance) 246 ($M^{\cdot+}$, 100), 231 (31). Anal. ($C_{17}H_{14}N_2$): C, H, N.

2l: Yield 70%, mp 239–241 °C. ^{1}H NMR δ 3.85 (s, 2H, CH_2), 7.2–8.4 (m, 9H, Ar, NH_2). MS: *m*/*z* (rel. abundance) 250 ($M^{\cdot+}$, 71), 102 (12), 77 (100), 63 (17). Anal. ($C_{16}H_{11}FN_2$): C, H, N.

2m: Yield 65%, mp >300 °C. ^{1}H NMR δ 3.9 (s, 2H, CH_2), 7.2–8.3 (m, 9H, Ar, NH_2). MS: *m*/*z* (rel. abundance) 266 ($M^{\cdot+}$, 56), 231 (76), 77 (100), 63 (37). Anal. ($C_{16}H_{11}ClN_2$): C, H, N.

11*H*-Indeno-[1,2-*b*]-quinolin-8,10-diamine 2b. A solution of **2a** (1.38 g, 0.005 mol) in tetrahydrofuran (100 mL) was hydrogenated at room temperature and room pressure over palladium on carbon. The reaction mixture was filtered from the catalyst and evaporated to dryness. The residue was crystallized from ethanol to yield 0.86 g (70%) of **2b** mp 150–152 °C dec. ^{1}H NMR δ 3.8 (s, 2H, CH_2), 5.15 (broad, 2H, NH_2), 6.2 (broad, 2H, NH_2), 7.0–8.0 (m, 7H, Ar). MS: *m*/*z* (rel. abundance) 247 ($M^{\cdot+}$, 14), 110 (11), 60 (100), 43 (74). Anal. ($C_{16}H_{13}N_3$): C, H, N.

11*H*-Indeno-[1,2-*b*]-quinolin-7,10-diamine 2d. With the same procedure and starting from **2c** (1.38 g, 0.005 mol) 0.5 g (40%) of **2d** mp >300 °C. ^{1}H NMR δ 3.8 (s, 2H, CH_2), 6.2 (broad, 2H, NH_2), 6.8–8.2 (m, 9H, Ar, NH_2). MS: *m*/*z* (rel. abundance) 247 ($M^{\cdot+}$, 100), 246 (13). Anal. ($C_{16}H_{13}N_3$): C, H, N.

***N*-(11*H*-Indeno-[1,2-*b*]-quinolin-10-yl)-benzylamine 2n.** A mixture of **1a** (1.0 g, 4.3 mmol), benzaldehyde (0.45 g, 4.3 mmol) in DMF (10 mL) and some molecular sieves was refluxed for 10 h. The reaction mixture was poured in ice and the obtained solid was collected by filtration, dried and purified by flash-chromatography (eluent: toluene/acetone 4:1). 0.25 g (20%) of Schiff base mp 152–154 °C were obtained. ^{1}H NMR δ 4.0 (s, 2H), 7.3–8.4 (m, 8H, Ar), 8.6 (s, 1H, CH).

To a methanolic solution of this compound a $NaBH_4$ solution (0.14 g in 2 mL of water) was added and the reaction mixture was stirred at room temperature for 10 h. The solvent was evaporated and the residue was taken up in methylene chloride. The solution was dried, evaporated and the residue was crystallized from toluene to give 0.10 g (50%) of **2n** mp 191–193 °C. ^{1}H NMR δ 4.2 (s, 2H, CH_2), 5.0 (d, 2H, CH_2), 5.25 (broad, 1H, NH), 7.3–8.3 (m, 13H, Ar). MS: *m*/*z* (rel. abundance) 322 ($M^{\cdot+}$, 43), 232 (34), 217 (6), 91 (100). Anal. ($C_{23}H_{18}N_2$): C, H, N.

10-Chloro-11*H*-indeno-[1,2-*b*]-quinoline 3. A mixture of anthranilic acid (13.7 g, 0.1 mol), 1-indanone (13.2 g, 0.1 mol) in phosphorus oxychloride (100 mL) was refluxed for 2 h. The reaction mixture was evaporated and treated with ice and $NaHCO_3$ solid. The separated solid was taken up in ether. The solution was washed with water, dried and evaporated. The residue was crystallized from petroleum ether to give 17.6 g (70%) of **3** mp 167–170 °C ^{1}H NMR δ 4.1 (s, 2H), 7.5–8.3 (m, 8H, Ar). Anal. ($C_{16}H_{10}ClN$): C, H, N.

***N*-(11*H*-Indeno-[1,2-*b*]-quinolin-10-yl)-methylamine 2o.** A mixture of **3** (0.75 g, 3 mmol) and 40% solution methylamine was heated at 170–180 °C in a Parr bomb for 10 h. The reaction mixture was taken up in water and the separated solid was collected by filtration, dried and purified by flash-chromatography (eluent: toluene:acetone 4:1) to give 0.08 g (10%) of **2o** mp 180–

182 °C. ^{1}H NMR δ 3.4 (d, 3H, CH_3), 4.3 (s, 2H, CH_2), 5.05 (broad, 1H, NH), 7.2–8.3 (m, 8H, Ar). MS: *m*/*z* (rel. abundance) 246 ($M^{\cdot+}$, 100), 231 (37), 216 (29), 122 (13). Anal. ($C_{17}H_{14}N_2$): C, H, N.

***N*-Heptyl-*N*-11*H*-indeno-[1,2-*b*]-quinolin-10-yl)-amine 2p.** With the same procedure and starting from **3** (0.75 g, 3 mmol), 0.1 g (10%) of **2p** mp 50–52 °C were obtained. ^{1}H NMR δ 0.9 (t, 3H, CH_3), 1.2–1.5 (m, 8H), 1.75 (m, 2H), 3.8 (t, 2H), 4.2 (s, 2H, CH_2), 7.4–8.3 (m, 8H, Ar). MS: *m*/*z* (rel. abundance) 330 ($M^{\cdot+}$, 59), 245 (100), 231 (21), 216 (14). Anal. ($C_{23}H_{26}N_2$): C, H, N.

2-Amino-4-nitrobenzonitrile. 2-Amino-4-nitrobenzoic acid (9.1 g, 0.05 mol) was refluxed with thionyl chloride (20 mL) for 24 h. The excess of $SOCl_2$ was evaporated under reduced pressure, the residue was solubilized with dioxane, and ammonia was bubbled for 2 h. The separated solid was collected by filtration to give 5.6 g (60%) of amide mp 207–210 °C, ^{1}H NMR δ 7.0–8.1 (m, 7H, Ar and NH_2). This compound was suspended with P_2O_5 (12 g) in toluene (400 mL) and the reaction mixture was refluxed for 15 h under stirring. After evaporation of the solvent, water was added and the separated solid was collected by filtration to give 3.6 g (90%) of product mp 193–195 °C. ^{1}H NMR δ 4.8 (broad, 2H, NH_2), 7.3–7.8 (m, 3H, Ar).

2-Amino-4-fluorobenzonitrile. With the same procedure and starting from 2-amino-4-fluorobenzoic acid, the amide (65%), mp 126–128 °C, ^{1}H NMR δ 6.2–7.8 (m, 7H, Ar and NH_2) and the nitrile (75%) mp 113–115 °C, ^{1}H NMR δ 4.55 (broad, 2H, NH_2), 6.4–7.45 (m, 3H, Ar) were obtained.

Enzyme kinetics

S-Acetylthiocholine iodide, *S*-butyrylthiocholine iodide 5,5′-dithio-bis-(2-nitrobenzoic) acid (DTNB, Ellman's reagent), acetylcholinesterase (0.5 U.I./mg) and butyrylcholinesterase (3.4 U.I./mg) derived from human erythrocytes were purchased from Sigma Chemical (Italy). Tacrine (9-amino-1,2,3,4-tetrahydroacridine hydrochloride) and propidium were obtained from Aldrich Italia. Buffer components and other chemicals were of the highest purity commercially available.

Inhibition of acetylcholinesterase and butyrylcholinesterase. The method of Ellman et al.[12] was followed. A 0.037 M ATCh iodide solution was prepared in water. 0.01 M 5,5′-Dithio-bis(2-nitrobenzoic) acid (Ellman' s reagent) was dissolved in pH 7.0 phosphate buffer and 0.15% (w/v) $NaHCO_3$ added. AChE solution was prepared dissolving 20 units in 5 mL of 0.2% aqueous gelatine by sonication at 35 °C. A dilution 1:1 with water was performed before use, in order to get the enzyme activity comprised between 0.130 and 0.100 AU/min. Stock solutions of the test compounds (1 mM) were prepared in methanol, as well as the tacrine and propidium reference stock solutions. The assay solutions were prepared by diluting the stock solutions in water. Five different concentrations of each compound were used, in order to obtain inhibition of AChE activity comprised between 20 and 80%.

The assay solution consisted of a 0.1 M phosphate buffer pH 8.0, with the addition of 340 μM DTNB, 0.035 unit/mL AChE derived from human erythrocytes, and 550 μM ACTh iodide. The final assay volume was 1 mL. Test compounds were added to the assay solution and preincubated with the enzyme for 20 min, the addition of substrate following.

Inhibition of BuChE was measured as described above, substituting 0.035 unit/mL of BuChE and 550 μM butyrylthiocholine iodide for enzyme and substrate, respectively.

Initial rate assays were performed at 37 °C with a Jasco Uvidec-610 double beam Spectrophotometer: the rate of increase of the absorbance at 412 nm was followed for 5 min. Assays were done with a blank containing all components except AChE and BuChE, in order to account for non-enzymatic reaction. The reaction rates were compared and the percent inhibition due to the presence of test compounds was calculated. Each concentration was analyzed in triplicate. The percent inhibition of the enzyme activity due to the presence of increasing test compound concentration was calculated by the following expression: $100-V_i/V_0\times100$ where V_i is the rate calculated in the presence of inhibitor and V_0 is the enzyme activity. Inhibition curves were obtained for each compound by plotting the percent inhibition versus the logarithm of inhibitor concentration in the assay solution. The linear regression parameters were determined for each curve and the IC_{50} values extrapolated. The same procedure was applied for the reference compounds tacrine and propidium.

Steady state kinetics. To obtain estimates of the competitive inhibition constant K_i for the compounds **1a**, **2n**, tacrine and propidium, reciprocal plots of $1/V$ versus $1/[S]$ were constructed at relatively low concentration of substrate (below 0.5 mM: Fig. 2a–d). The plots were assessed by a weighted least square analysis that assumed the variance of V to be a constant percentage of V for the entire data set. Slopes of these reciprocal plots were then plotted against the inhibitor concentrations (Fig. 2e–h) in a similar weighted analysis, and K_i values were determined as the ratio of the replot intercept to the replot slope.

Computational methods

Molecular dynamics (MD) simulations were performed using the united-atom AMBER* force field implemented in the MacroModel Ver. 5.5 program[23], running on a Silicon Graphics Indigo2 workstation. The SYBYL molecular modeling package[24] was used for the initial docking of **1a**. The coordinates of the tacrine–AChE complex were obtained from the X-ray structure determined using AChE isolated from *T. californica*[10] and were retrieved from the Brookhaven Protein Data Bank (entry 1acj); Phe330 was replaced by Tyr with the same conformation. Polar and aromatic hydrogens were added to the protein, while the aliphatic portions of the macromolecule were treated using the united-atom model of AMBER[25]. The water molecules present in the

PDB file were maintained in their original positions, and were subjected to the simulation studies. The inhibitor **1a** was built by properly modifying the structure of tacrine and docked into the enzyme active site in such a way as to avoid unfavorable contacts.

An MD protocol[26] was applied to study the behavior of **1a** in the active site pocket. A core of atoms around the active site and a shell surrounding the core were defined, on which the minimizations and the dynamics simulations were carried out. The core was made up by any atom of the protein within 8 Å from any atom of the inhibitor; the shell contained any atom within 6 Å from any atom of the core. All the atoms within the core were unconstrained, while atoms in the shell were constrained by applying an energy penalty force constant of 100 kJ/Å^2 mol^{-1}. Atoms beyond the shell were maintained at the X-ray coordinates. On such a system, an initial minimization (2000 steps, steepest descent) and a subsequent temperature constant MD simulation (140 ps, 298 K, 1.0 fs time step) were carried out. An equilibration time of 60 ps was allowed before starting the data collection. The SHAKE algorithm[27] was used to constrain all bonds involving hydrogens at their equilibrium values. The MD average structure of the last 80 ps was energy minimized first by steepest descent (3000 steps) and then by conjugate gradient with a derivative convergence criterion of 0.05 kJ/Å^2 mol^{-1}.

Acknowledgements

Investigation supported by University of Bologna (funds for selected research topics) and by MURST.

References

1. Bartus, R. T. *Science* **1982**, *217*, 408.
2. Gualtieri, F.; Dei, S.; Manetti, D.; Romanelli, M. N.; Scapecchi, S.; Teodori, S. *Il Farmaco* **1995**, *50*, 489.
3. Diaz Brinton, R.; Yamazaki, R. S. *Pharm. Res.* **1998**, *15*, 386.
4. Parnetti, L.; Senin, U.; Mecocci, P. *Drugs* **1997**, *53*, 752.
5. Cheng, X.-M. *Ann. Rep. Med. Chem.* **1994**, *29*, 331.
6. Valenti, P.; Rampa, A.; Bisi, A.; Andrisano, V.; Cavrini, V.; Fin, L.; Buriani, A.; Giusti, P. *Bioorg. Med. Chem. Lett.* **1997**, *7*, 2599.
7. McKenna, M.; Proctor, G. R.; Young, L. C.; Harvey, A. L. *J. Med. Chem.* **1997**, *40*, 3516.
8. Inestrosa, N. C.; Alvarez, A.; Perez, C. A.; Moreno, R. D.; Vicente, M.; Linker, C.; Casanueva, O. I.; Soto, C.; Garrido, J. *Neuron* **1996**, *16*, 881.
9. Schenk, D. B.; Rydel, R. E.; May, P.; Little, S.; Panetta, J.; Lieberburg, I.; Sinha, S. *J. Med. Chem.* **1995**, *38*, 4141.
10. Sussman, J. L.; Harel, M.; Silman, I. *Chem.–Biol. Interact.* **1993**, *87*, 187.
11. Soreq, H.; Ben-Aziz, R.; Prody, C. A.; Seidman, S.; Gnatt, A.; Neville, L.; Lieman-Hurwitz, J.; Lev-Lehman, E.; Ginzberg, D.; Lapidot-Lifson, Y.; Zakut, H. *Proc. Natl. Acad. Sci. USA* **1990**, *87*, 9688.
12. Ellman, G. L.; Courtney, K. D.; Andres, V.; Featherstone, R. M. *Biochem. Pharmacol.* **1961**, *7*, 88.
13. Shutske, G. M.; Pierrat, F. A.; Kapples, K. J.; Cornfeldt, M. L.; Szewczak, M. R.; Huger, G. M.; Bores, G. M.; Haroutunian, V.; Davis, K. L. *J. Med. Chem.* **1989**, *32*, 1805.
14. Wlodek, S. T.; Antosiewicz, J.; McCammon, J. A.; Straatsma, T. P.; Gilson, M. K.; Briggs, J. M.; Humblet, C.; Sussman, J. L. *Biopolymers* **1996**, *38*, 109.
15. Hansch, C.; Leo, A.; Hoekman, D. *Exploring QSAR. Hydrophobic, Electronic and Steric Constants*; ACS Professional Reference Book; American Chemical Society: Washington, DC, 1995.
16. Steinberg, G. M.; Mednick, M. L.; Maddox, J.; Rice, R. *J. Med. Chem.* **1975**, *18*, 1056.
17. Recanatini, M.; Cavalli, A.; Hansch, C. *Chem.–Biol. Interact.* **1997**, *105*, 199.
18. Radic, Z.; Reiner, E.; Taylor, P. *Mol. Pharmacol.* **1990**, *39*, 98.
19. Krupka, R. M.; Laidler, K. J. *J. Am. Chem. Soc.* **1961**, *83*, 1454.
20. Massoulié, J.; Sussman, J.; Bon, S.; Silman, I. *Progr. Brain Res.* **1993**, *98*, 139.
21. Fersht, A. *Enzyme Structure and Mechanism*; W. H. Freeman and Co.: New York, 1985; Chapter 3.
22. Ping Pang, Y.; Quiram, P.; Jelacic, T.; Hong, F.; Brimijoin, S. *J. Biol. Chem.* **1996**, *271*, 23646.
23. Mohamadi, F.; Richards, N. G. J.; Guida, W. C.; Liskamp, R. M. J.; Lipton, M. A.; Caulfield, C. E.; Chang, G.; Hendrickson, T. F.; Still, W. C. *J. Comput. Chem.* **1990**, *11*, 440.
24. SYBYL; version 6.4; Tripos Ass.: St. Louis, MO.
25. Weiner, S. J.; Kollman, P. A.; Case, D. A.; Singh, U. C.; Ghio, C.; Alagona, G.; Profeta, Jr., S.; Weiner, P. *J. Am. Chem. Soc.* **1984**, *106*, 765.
26. Rampa, A.; Bisi, A.; Valenti, P.; Recanatini, M.; Cavalli, A.; Andrisano, V.; Cavrini, V.; Fin, L.; Buriani, A.; Giusti, P. *J. Med. Chem.* **1998**, *41*, 3976.
27. Ryckaert, J. P. *Mol. Phys.* **1985**, *55*, 549.